DIRECT CATALYTIC SYNTHESIS OF ACETIC ACID FROM CO_2 AND CH_4

Principal Investigator: Naomi Klinghoffer

Gas Technology Institute
1700 S. Mt. Prospect Rd.
Des Plaines, IL 60018
GTI Project No. 21600

Email: naomi.klinghoffer@gastechnology.org

CCEMC Project Advisor: Shunlan Liu

CCEMC Project #: K130108

Project Completed: Sept. 30th, 2016

Total CCEMC funds: $500,000 CAD

Submission date: Oct. 14th, 2016

Contents

1 Executive Summary

This project investigated production of acetic acid (CH_3COOH, CAS Registry Number: 64-19-7), which is a heavily produced commodity chemical, from CO_2 and CH_4. Acetic acid is a versatile intermediate chemical, used in a variety of products, such as paints, adhesives and solvents, as well as in the production of purified terephthalic acid (PTA) for polyester manufacturing. GTI proposed a new route for producing acetic acid based on the direct catalytic reaction of methane with carbon dioxide. First, CH_4 is adsorbed on the surface of the catalyst and dissociated to generate a surface carbonaceous Metal-CH_x species. Next, CO_2 is inserted into the Metal-CH_x bond. Finally, hydrogenation of the intermediates yields acetic acid and returns the catalyst to the metal. The stepwise reaction takes place isothermally. The catalyst used contained palladium and cobalt on a silica support. The second method investigated was dry reforming of methane (by reaction with CO_2) to produce syngas, which is a precursor to methanol, formic acid, and acetic acid. For this reaction, a nickel based catalyst was used on a stable support, and was synthesized using atomic layer deposition methods. Experiments were done at reaction temperatures between 700-850^oC. A methane reforming rate >2000 L h^{-1} g_{cat}^{-1} was achieved. Deactivation testing suggested that catalyst performance could be recovered by regeneration.

Keywords: Dry reforming, nickel catalyst, CO_2 utilization, catalyst regeneration

2 Project Description

2.1 Direct synthesis of acetic acid

The proposed technology aimed to synthesize acetic acid (CH_3COOH, CAS Registry Number: 64-19-7), which is a heavily produced commodity chemical, from CO_2 and CH_4. Acetic acid is a versatile intermediate chemical, used in a variety of products, such as paints, adhesives and solvents, as well as in the production of purified terephthalic acid (PTA) for polyester manufacturing. The most frequently used route of production is the Cativa process.[1] This process involves methanol carbonylation under catalytic conditions. The main chemical reaction is as follows:

$$CH_3OH + CO \rightarrow CH_3COOH$$

GTI proposed a new route for producing acetic acid based on the direct catalytic reaction of methane with carbon dioxide. First, CH_4 is adsorbed on the surface of the catalyst and dissociated to generate a surface carbonaceous Metal-CH_x species. Next, CO_2 is inserted into the Metal-CH_x bond. Finally hydrogenation of the intermediates yields acetic acid and returns the catalyst to the metal. The stepwise reaction takes place isothermally. The reaction proceeds as follows:

The balance of the first step:

$$CH_4 + \text{Metal} \rightarrow \text{Metal-}CH_x + \tfrac{1}{2}(4 - x)\, H_2 \; (x = 0 - 3, \text{ moles } H_2 \text{ evolved})$$

The balance of the second step:

$$CO_2 + \text{Metal-}CH_x + \tfrac{1}{2}(4 - x)\, H_2 \text{ (supplied)} \rightarrow CH_3COOH + \text{Metal}$$

The total balance:

$$CH_4 + CO_2 + \tfrac{1}{2}(4 - x)\, H_2 \text{ (supplied)} \rightarrow CH_3COOH + \tfrac{1}{2}(4 - x)\, H_2 \text{ (evolved)}$$

Acetic acid was to be produced by the above mentioned route. A near equal amount of ethanol (C_2H_5OH, CAS Registry Number: 64-17-5) was to be produced by coupling of two Metal-CH_x species and reaction with H_2O. Due to poor conversion from this one step approach (discussed in Section 3), we focused our work on using CO_2 for dry reforming of methane in order to produce synthesis gas/syngas ($CO + H_2$), which is a feedstock for the traditional two step process for acetic

acid synthesis. In the traditional process, syngas is used to produce methanol, which subsequently reacts with carbon monoxide (CO) to produce acetic acid. By using synthesis gas made from CO_2 and CH_4, acetic acid can be produced with half of the carbon coming from CO_2, thus utilizing CO_2 in the chemical industry rather than releasing it to the atmosphere.

2.2 Dry reforming of methane with CO_2

The dry reforming of methane (DRM) reaction is the reaction of CO_2 with CH_4 to produce syngas, as shown below.

Dry reforming of methane: $CO_2 + CH_4 \rightarrow 2\ CO + 2\ H_2$

This reaction requires high reaction temperature (typically higher than 700ºC), and typically takes place at atmospheric pressure. In conventional DRM, the supported metal catalysts often experience deactivation due to sintering (from high temperature) and coking. Thus, it is desirable to develop a thermally stable catalyst which can resist sintering and coking.[2,3] Different metal catalysts (e.g., Rh,[4] Pt,[5] Pd,[6] Ru,[7] and Ni[8]) have been employed to catalyze the DRM reactions. Ru and Rh were demonstrated to have the highest activity among these metal catalysts.[9] The Ni-based catalysts showed lower resistance to coking, as compared to noble metal based catalysts.[10] However, due to the limited availability and high cost of noble metals, it is more desirable to develop a Ni-based catalyst with higher thermal stability and resistance to coking and sintering.

Noble metal and Ni catalysts are normally prepared by an impregnation method. The metal nanoparticles prepared by that method generally have issues of lower catalytic activity and severe coke formation (activity loss) due to their large particle size (e.g., 10-30 nm or larger), and low thermal stability due to a weak interaction between the metal nanoparticles and the catalyst support. The addition of promoters have been reported to be favorable for increasing metal-support interaction. For example, Wang et al. reported that the addition of a CeO_2 promoter into the Rh/Al_2O_3 catalyst improved the performance of the catalysts in DRM.[11] These promoters were conventionally added by a liquid phase impregnation method, in which the loading and location of the promoters were difficult to control and led to high loading that could block the catalytic sites.

Atomic layer deposition (ALD) is a self-limiting and self-terminating gas phase deposition technique that has been successfully demonstrated for the deposition of different films and metal nanoparticles, that are chemically bonded to substrates.[12, 13] ALD thin film coating has already been commercialized in the semiconductor industry. ALD thin film coating on particles that range from a few nanometers to micron size in diameter can be carried out in fluidized bed reactors, which are inherently scalable and provide for intimate contact between solids and gases.[14] The ALD technique has been employed to synthesize highly stable and active Ni catalysts and to load them onto porous support substrates. The loading of metal catalysts can be precisely controlled. For example, we very recently reported in *Applied Catalysis B: Environmental* (vol. 201, pp.302-309) that porous γ-Al_2O_3 particles-supported Ni nanoparticle catalyst prepared in our laboratory using the ALD technique showed extremely high methane reforming rates at different temperatures (1840 $Lh^{-1}g_{Ni}^{-1}$ at 850 °C, 1740 $Lh^{-1}g_{Ni}^{-1}$ at 800 °C, 1320 $Lh^{-1}g_{Ni}^{-1}$ at 750 °C).[15] These are the highest DRM reaction rates reported to date as compared to data in the literature. The porous alumina particles used in our study were 40 μm in diameter with a Brunauer−Emmett −Teller (BET) surface area of ~100 m^2/g.

3 Outcomes and Learnings

3.1 Acetic acid synthesis

3.1.1 Reactor design

Construction of simulated moving bed test system

The steps in the process follow this proposed reaction mechanism:

Step 1: $CH_4 + (5-x)M \longrightarrow M-CH_x + (4-x)M - H$

Step 2: $M-CH_x + O=C=O \longrightarrow M-O-CO-CH_x$

$$M-O-CO-CH_x + (4-x)M - H \longrightarrow CH_3COOH + (5-x)M$$

In the first step, CH_4 adsorbs onto the catalyst surface and dissociates. In the second step, CO_2 reacts with the adsorbed CH_x. To simulate a continuous reactor design, the system has two reactors, each containing the same catalyst, where the CO_2 and CH_4 gas streams are cycled from one reactor to the other. When Reactor 1 is in step 1, Reactor 2 is in step 2. After a predetermined amount of time the inlet gas streams are switched to the reactors. This introduces step 2 conditions

to reactor one and step one conditions to reactor 2. At the same time the outlet streams are switched to keep the gas sampling equipment on the exit of the second step, sampling for CH_3COOH. This cycle of reactor switching is done continuously until the end of testing. Figure 1 shows the process flow diagram for the setup. Steam is added based on the literature which suggests that the presence of steam improves activity.[17]

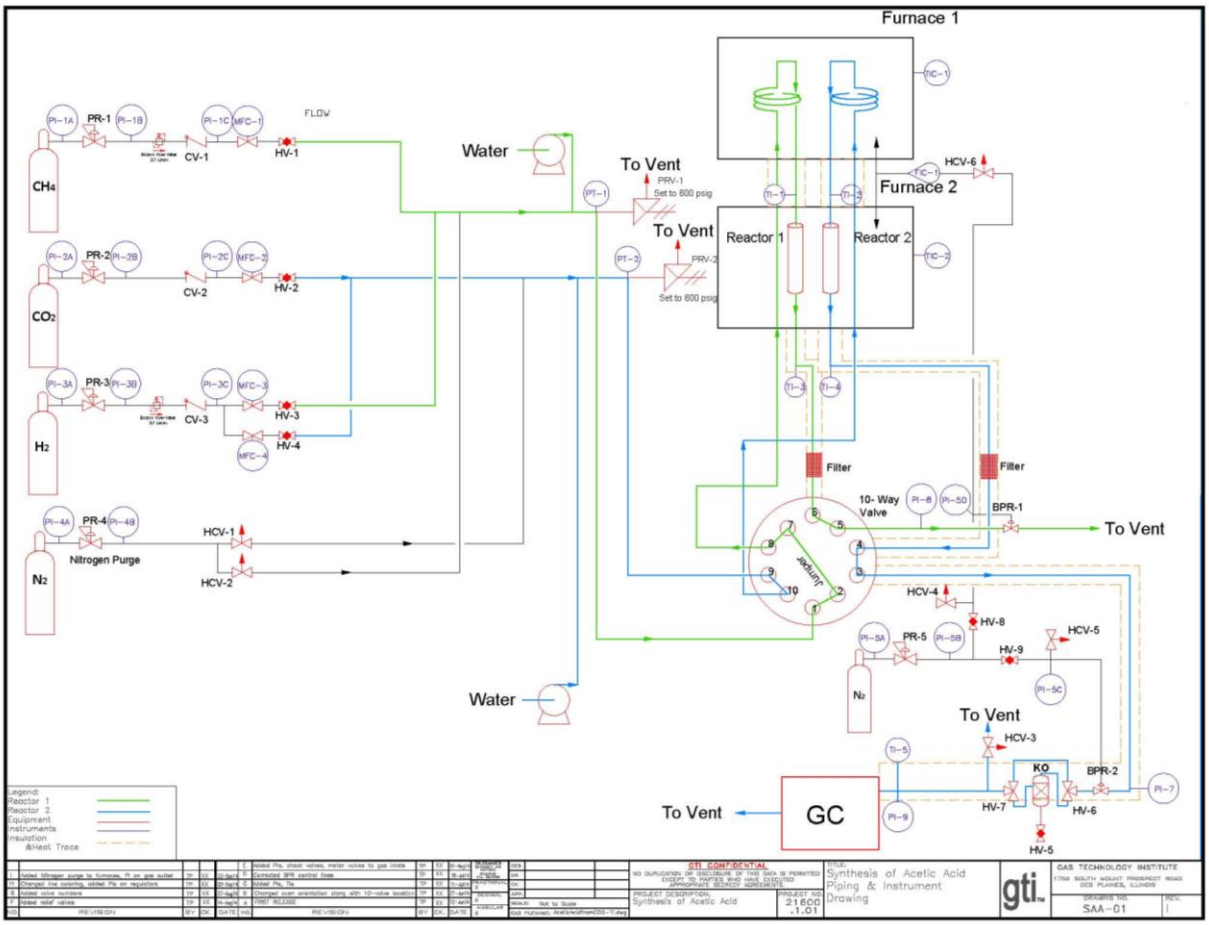

Figure 1. Simulated moving-bed reaction process flow diagram.

The main parts of the test equipment are:

1. Gas Inlet Mixer
    - Mass Flow controllers
    - High pressure low flow liquid pumps
    - Pressure transducers
    - Pressure Relief Valves
2. Reactors and Heaters
    - Two Reactors

- Two heating zones
- Gas preheating coils

3. Outlet and Analysis
    - Diaphragm back pressure control valves
    - Agilent Micro GC for gas analysis
    - Liquid knock out vessel
4. VICI 10-port two position valve
    - Allows simultaneous switching of inlet and outlet lines from one reactor to the other

Gas Inlet Mixer

The setup has two main ¼" stainless steel inlet gas lines. Line one, shown in green color in Figure 1, mixes gases and steam for the first step in the proposed reaction mechanism. CH_4 and H_2 are fed using Brooks mass flow controllers (MFC) and steam is generated using liquid water injection into the heated gas inlet line. A high pressure low flow liquid pump, manufactured by Eldex, is used to introduce water.

Line two, shown in blue, mixes gases and steam for the second step. CO_2 and H_2 are mixed using Brooks MFCs and water is injected using an Eldex pump similar to step 1. Each line has a pressure transducer and a pressure relief valve. In addition to the reaction gases, each line has a N_2 purge line. This allows inert gas flow (that is mixed with H_2) during the catalyst activation step before conversion testing. Nitrogen flow is also used during startup and shutdown. Figure 2 shows a picture of the experimental setup in GTI's Gas Processing Lab.

Figure 2. Picture of the experimental setup.

Reactors and Heaters

There are two 5KW heaters in the setup. Heater 1 (above Heater 2) preheats feed gases and Heater 2 houses the reactors. The two inlet lines enter Heater 2 from the bottom, travel through and enter Heater 1 where they are connected to the preheater coils. The preheater coils are about 10 ft. of ¼" stainless steel tubing coils with 4" diameter. The lines then continue down back to Heater 2 and are connected to Reactor 1 and 2. Reactors are made from ½" stainless steel tubing. The reactors are 16 inches long and allow the catalyst bed be placed at various desired locations. The gas lines exit the reactors at the bottom of Heater 2. Through a "T" fitting at the bottom, thermocouples are inserted to each reactor. The tip of the thermocouple sits inside the catalyst bed. There are thermocouples inserted into the gas lines between the two heaters to measure the temperature of the gases entering the reactors. To ensure safe operation, there are control and over-temperature protection thermocouples for each heater. The interior volume of the heaters is purged with N_2 to prevent high concentrations of H_2 buildup in the event of a leak. Figure 3 shows a picture of the reactors in Heater 2.

Figure 3. Photo of the reactors.

Outlet and Analysis

The outlet gas lines from the reactors are plumbed to follow two separate directions. In normal operating mode, the outlet from reactor that is in step 1 of the reaction cycle is vented without analysis. The outlet from the reactor that is in step 2 and producing acetic acid is sent to the Agilent micro-GC for analysis. If desired, the outlet flow path could be switched so that the outlet of step 1 flows to the micro-GC and the outlet from step 2 is vented. The outlet line for analysis also includes a liquid knock out (KO) vessel. Total flow from the reactor can either be directed to the KO vessel or bypassed around it. Then a slip steam is sent to the micro GC for sampling. A Genie membrane filter, manufactured by Aplus Corp., is in place to protect the micro GC from any condensed liquids that may be in the sample line. The GC method is created for analysis of permanent gases and acetic acid and ethanol vapors. The GC is calibrated for permanent gases, acetic acid and ethanol.

10-Port valve

The simultaneous switching of inlet and outlet streams between reactors is done by using a VICI 10-port dual position rotary valve. With one rotation both the inlets and the outlets from both reactors are switched. Figure 4 shows a picture of the 10-port valve and the inlet & outlet tubing.

Figures 5 and 6 show plumbing diagrams for the inlet and outlet connections at valve positions A and B.

Figure 4. Picture of the 10-port valve and associated tubing.

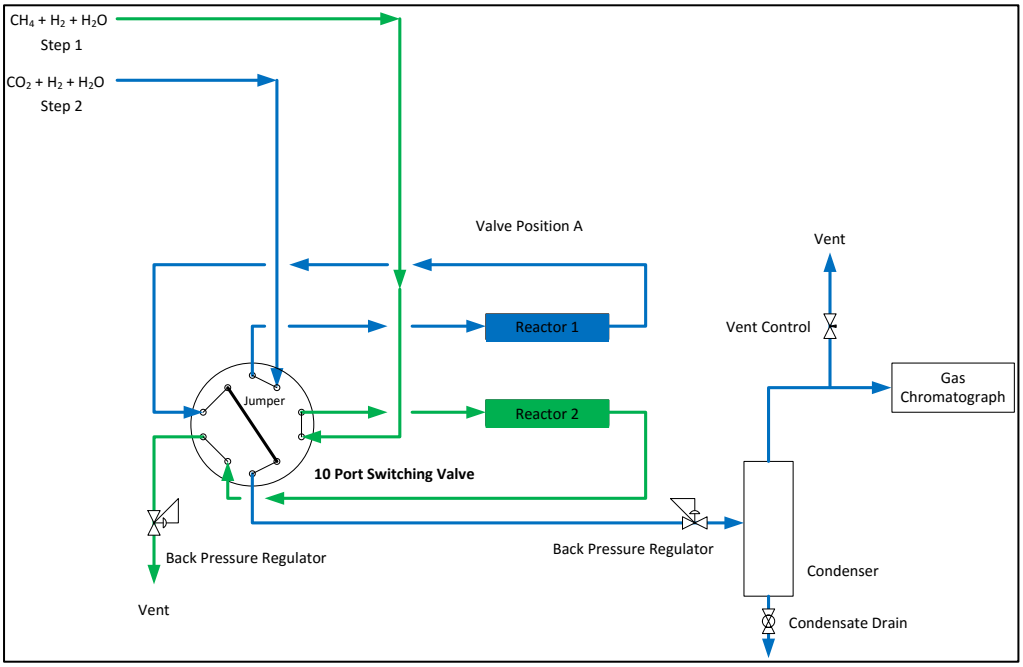

Figure 5. Diagram for VICI 10-Port valve position A.

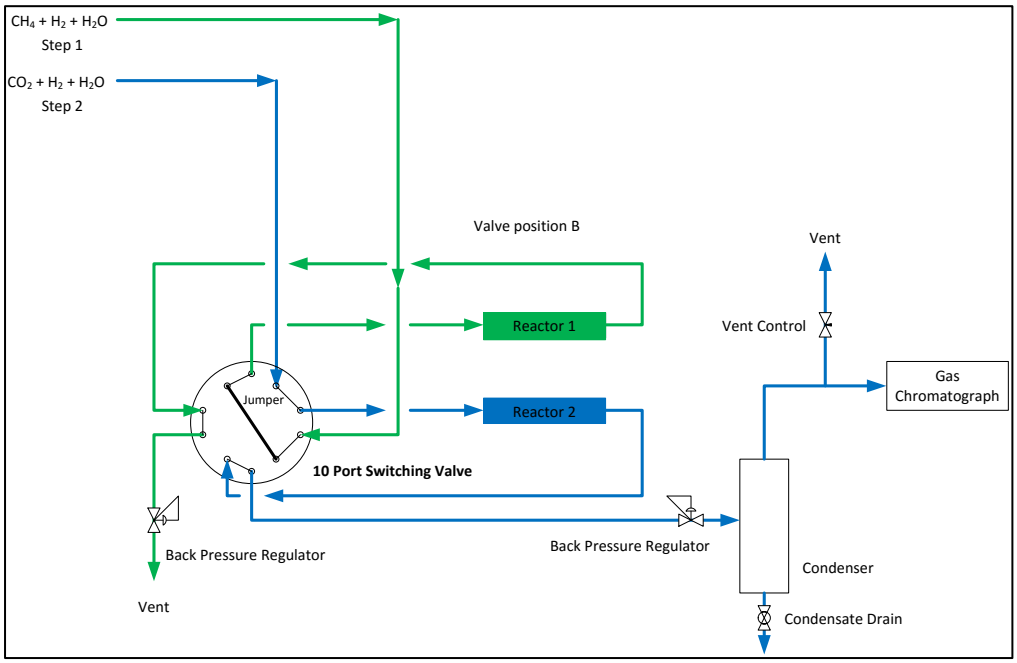

Figure 6. Diagram for VICI 10-Port valve position B.

LabVIEW Control

The data acquisition and control of the setup is done by a custom made LabVIEW program running on a PC. The PC communicates with a data acquisition and control hardware, manufactured by National Instruments, to read temperature, pressure and flow data. In addition to collecting data, the hardware also controls MFCs and heaters. The program is also capable of timing and control of the 10-port valve to cycle the reactors between steps 1 and 2 flow conditions. All data acquired from the setup and all control signals sent to the setup are logged and saved to the computer. Figure 7 shows a picture of the control software and computer.

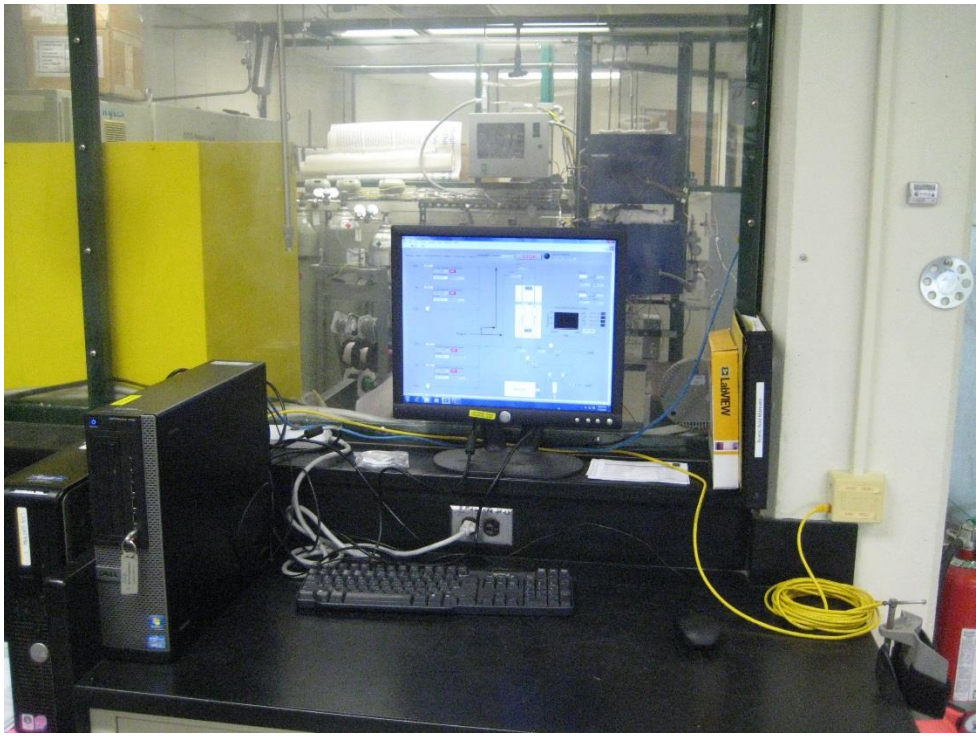

Figure 7. Picture of the LabVIEW control software and the control PC.

Safety

GTI's engineering staff conducted a hazard and operability study (HAZOP) to insure the safety and operability of the acetic acid synthesis system. Also, standard operating procedures for experiments and catalyst synthesis (discussed below) were developed and reviewed. Before each test, the system was pressure-checked to ensure there were no leaks. The process control software was set up to automatically shut down in the case of high temperature events. There were no safety issues related to this project during the program.

3.1.2 Catalyst synthesis

Based on a literature search, catalysts containing Ru, Pd, Pt, Co and Ni can be active in acetic acid synthesis. Ru or Ni are more active for methane dissociation compared to Pd or Pt, which have similar activity for methane activation: total dissociation energies for complete dissociation with Ru and Ni are smaller than for Pd and Pt.

Catalysts were synthesized with the wet impregnation method. Different metal precursors (platinum nitrate, cobalt nitrate, palladium chloride, and ruthenium nitrosyl nitrate) were used. Various supports for catalyst such as silica and titanium dioxide were tested. A catalyst with composition 3% Pd-6%Co/TiO_2 (weight percentage) was synthesized as follows. First palladium chloride was dissolved in water with the addition of a small amount of hydrochloric acid to help it dissolve. Next, the titanium dioxide support was impregnated with the solution. The sample was dried at 343K for 2 hours and calcined at 773K for 4 hours. The sample was then impregnated with aqueous solution of cobalt nitrate and drying and calcinations was repeated. Various catalysts were synthesized with different compositions using the same technique. Each catalyst design was based on observations reported in the literature, and is described below.

The following catalysts were synthesized:

1. 6% Co/3% Pd on TiO_2:

   Rationale: This catalyst was made in order to reproduce that which was reported in the literature.[17]

   Synthesis procedure: The procedure reported in [17] was followed: first a TiO_2 support was impregnated with a palladium chloride solution. Second, the catalyst was dried at 70°C for 2 hours and calcined at 500°C for 4 hours. Finally, it was then impregnated with an aqueous cobalt nitrate solution and calcined and dried at the same conditions.

2. 6% Co/3% Pd on SiO_2:

   Rationale: A silica support was used based on the reported literature which indicated that silica is a good support for metal catalysts which are used for methane activation and homologation.[18] When cobalt was supported on silica, the methane conversion was reported to be two orders of magnitude higher than when titania or alumina supports were used. With a palladium catalyst, methane conversion was 20% higher on silica compared to titania.

   Synthesis procedure: A SiO_2 support was impregnated with a palladium chloride solution using incipient wetness technique. The catalyst was dried at 120°C for 2 hours and calcined at 500°C for 4 hours. It was then impregnated with an aqueous cobalt nitrate solution and calcined and dried at the same conditions.

3. 6% Co/3% Pt on SiO_2:

   Rationale: A platinum catalyst was used in place of palladium based on the reported literature which indicated that platinum had higher activity than palladium for methane activation and homologation.[18]

   Synthesis procedure: A SiO_2 support was impregnated with a platinum nitrate solution using incipient wetness technique. The catalyst was dried at 120°C for 2 hours and calcined at 500°C for 4 hours. It was then impregnated with an aqueous cobalt nitrate solution and calcined and dried at the same conditions.

4. 6%Co/1%Mg/3%Pd on SiO_2:

   Rationale: Magnesium has been shown to have activity for methane activation.[19]

   Synthesis procedure: A SiO_2 support was impregnated with a solution containing cobalt nitrate and magnesium nitrate hexahydrate using incipient wetness technique. The catalyst was dried at 120°C for 2 hours and calcined at 500°C for 4 hours. It was then impregnated with an aqueous palladium chloride solution and calcined and dried at the same conditions.

5. Co/Ru on SiO_2:

   Rationale: Ruthenium was used in place of palladium since ruthenium has been shown to have activity for conversion of methane to higher hydrocarbons in an oxygen free environment.[20]

   Synthesis procedure: A SiO_2 support was impregnated with a solution a solution containing cobalt nitrate using incipient wetness technique. The catalyst was dried at 120°C for 2 hours and calcined at 500°C for 4 hours. It was then impregnated with an aqueous ruthenium nitrosyl solution and calcined and dried at the same conditions.

Surface area:

The surface area of each catalyst was measured to verify that catalysts retained high surface area after preparation, since calcination exposed materials to high temperatures (500^{o}C). Results are shown in Table 1. All catalysts had acceptable surface areas. The surface area of titania was lower than silica (83 compared to 241-273 $m^2\ g^{-1}$). The surface area of one of the used catalysts was measured and was shown to be lower than the fresh catalyst (181 vs 273 $m^2\ g^{-1}$), indicating possible catalyst deactivation.

Table 1. BET surface area of catalysts synthesized. All catalysts are unused unless otherwise indicated.

Catalyst	**BET surface area (m^2g^{-1})**
Pt-Co/SiO_2	273
Pt-Co/SiO_2 (used)	181
Pd-Co/SiO_2	259
Pd-Co/TiO_2	83
Ru-Co/SiO_2	264
Pd-Co-Mg/SiO_2	241

3.1.3 Catalyst testing

Experimental procedure

The experimental procedure is as follows. The reactors are each charged with 2g of powder catalyst which is supported on a quartz wool bed. The system is then leak checked at a pressure that is higher than the operating pressure for that test. The catalysts are reduced at atmospheric pressure, in 10% H_2 in N_2 at 400°C for at least 3 hours. The reactor is then cooled down to the reaction temperature, or left overnight under nitrogen.

For every test, the first step is to introduce nitrogen flow to both reactors. The reactors are then pressurized and heated to desired set points. Once stable conditions are achieved, CH_4 and CO_2 are introduced into reactors 1 and 2 respectively, and N_2 flow is decreased. H_2 and water are then introduced to both reactors. Gas samples are drawn from the CO_2 line to the micro GC for analysis. Once the system reaches steady state, as determined by steady readings with the micro GC, the ten port valve is switched so that CO_2 and CH_4 are introduced to the alternate reactor. Valve switching can be done manually or automatically at a set frequency. During initial tests, gas samples were taken with a syringe and injected into the GC/MS for analysis. Later, the GC/MS was installed on-line so samples were sent through a 1/16" OD tube directly to the GC/MS for analysis of products.

Results and Discussion

Experiments were conducted on the test rig shown in Figure 1. Table 2 shows the conditions for the tests performed. The switch time indicates the amount of time that the 10-port valve was in one position.

Table 2. Conditions for each test performed.

Test #	**Catalyst**	**Temp R1 (ºC)**	**Temp R2 (ºC)**	**Pressure (psig)**	**Flow Rates (mL min^{-1})**								**switch time (s)**
					CH_4	**H_2**	**H_2O**	**N_2**	**CO_2**	**H_2**	**H_2O**	**N_2**	
1	Pd/Co/TiO_2	166	166	150	70	7	0.01	15	70	7	0.01	15	900
2	Pd/Co/TiO_2	166	166	150	70	7	0.01	15	70	7	0.01	15	200
3	Pd/Co/TiO_2	166	166	50	70	7	0.01	15	70	7	0.01	15	200
4	Pd/Co/TiO_2	166	166	50	70	7	0.01	15	70	7	0.01	15	300
5	Pd/Co/TiO_2	166	166	50	50	5	0	15	50	5	0	15	300
6	Pd/Co/TiO_2	166	166	50	50	5	0	0	50	5	0	0	400
7	Pd/Co/TiO_2	166	166	atm	50	0	0	0	50	5	0	0	200
8	Pt/Co/SiO_2	175	195	atm	70	7	0.01	15	70	7	0.01	15	180
9	Pt/Co/SiO_2	175	195	atm	70	7	0.01	15	70	7	0.01	15	200
10	Pt/Co/SiO_2	150	150	atm	50	5	0	15	50	5	0	15	200
11	Pt/Co/SiO_2	140	175	atm	50	5	0	15	50	5	0	15	120
12	Pt/Co/SiO_2	150	150	atm	50	5	0	15	50	5	0	15	60
13	Pt/Co/SiO_2	170	190	40	50	5	0	15	50	5	0	15	60
14	Pt/Co/SiO_2	235	260	50	70	7	0	15	70	7	0	15	900
15	Pt/Co/SiO_2	235	260	50	70	7	0.01	15	70	7	0.01	15	900
16	Pt/Co/SiO_2	235	260	100	70	7	0.01	15	70	7	0.01	15	900
17	Pt/Co/SiO_2	235	260	100	70	0	0.01	15	70	7	0.01	15	900
18	Pt/Co/SiO_2	235	260	100	70	0	0.01	15	70	7	0.01	15	60
19	Pd/Co/SiO_2	250	250	110	70	7	0.01	0	70	0	0.01	0	60
20	Pd/Co/SiO_2	250	250	110	0	0	0.01	70	70	7	0.01	0	60
21	Pd/Co/SiO_2	280	280	200	70	7	0.01	15	70	7	0.01	15	2400
22	Pd/Co/SiO_2	300	300	200	70	7	0.01	15	70	14	0.01	15	1800
23	Pd/Co/SiO_2	330	330	250	70	0	0	15	70	14	0	15	1800
24	Pd/Co/SiO_2	330	330	250	70	0	0.01	15	70	14	0.01	15	1800
25*	Pd/Co/Mg/SiO_2	400	400	150	167	17	0.01	15	167	17	0.01	15	900
26*	Pd/Co/Mg/SiO_2	400	400	100	167	17	0.01	15	167	17	0.01	15	900
27*	Pd/Co/Mg/SiO_2	400	400	50	167	17	0.01	15	167	17	0.01	15	900
28*	Ru/Co/SiO_2	400	400	150	167	17	0.01	15	167	17	0.01	15	900
29*	Ru/Co/SiO_2	400	400	100	167	17	0.01	15	167	17	0.01	15	900
30*	Ru/Co/SiO_2	400	400	50	167	17	0.01	15	167	17	0.01	15	900

**in these tests, reactors were charged with 5g of catalyst instead of 2g*

Some tests showed production of ethanol at concentrations up to 177 ppm, corresponding to a yield of 0.9 mg $(g_{cat}\ h)^{-1}$. Methanol was also detected. Various small peaks were detected in the CP-Sil column of the micro GC, which is used for detection of gases with a carbon number greater than 2. Production of these compounds corresponded to reaction conditions (i.e., they are produced in the stream containing CO_2), however, concentrations were too low to identify with certainty what the compounds were. They were likely hydrocarbons with carbon number greater than 2. When the methane stream was replaced with nitrogen these peaks were not observed, indicating that methane participates in this reaction. An example of test data from test #24 is shown in Figures 8 and 9. There is a tradeoff between CH_4 and CO_2, indicating when the valve has been switched, the CH_4 is purged out of the reactor and replaced with CO_2. Products are visible with the CO_2 stream. In this test, one reactor contained a $Pd/Co/SiO_2$ catalyst and the other reactor (in parallel) was empty. The results from cycles 2 and 4 are from the reactor containing the catalyst, and cycles 1 and 3 pass through the empty reactor. This clearly indicates the role of the catalyst. In the cycles where the micro GC is sampling from the empty reactor, no products are formed. With the catalyst, products are formed, and H_2 concentration is lower, indicating that hydrogen participates in the reaction. Ethanol and ethylene were observed in the micro GC data. We used the online GC/MS, in order to verify the chemical composition of all minor products.

Assuming ethylene and ethanol are each derived from one mole of CH_4 and one mole of CO_2, the conversion of CO_2 or CH_4 to ethylene and ethanol is calculated to be 0.34%. Methanol was also detected. The flow rate of CO_2 into the reactor was 70.0 mL/min, and the flow out of the reactor was calculated to be 65.4 mL/min (using nitrogen as an inert internal standard), giving an overall CO_2 conversion of 6.5%. However, 69% of the total CO_2 converted resulted in the production of methane, which is not desirable. CO was detected in the products as well, correlating to approximately 1.5% conversion of CO_2 to CO.

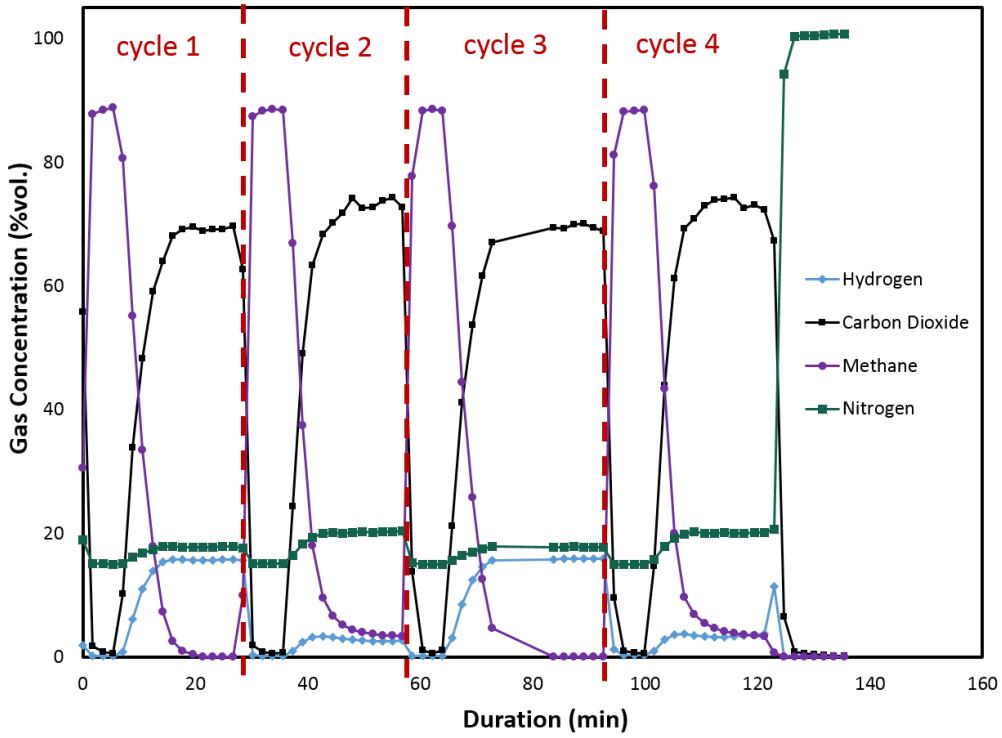

Figure 8. Major components from process. Cycles 2 and 4 pass through a Pd/Co on SiO_2 catalyst. Cycles 1 and 3 pass through a reactor with no catalyst.

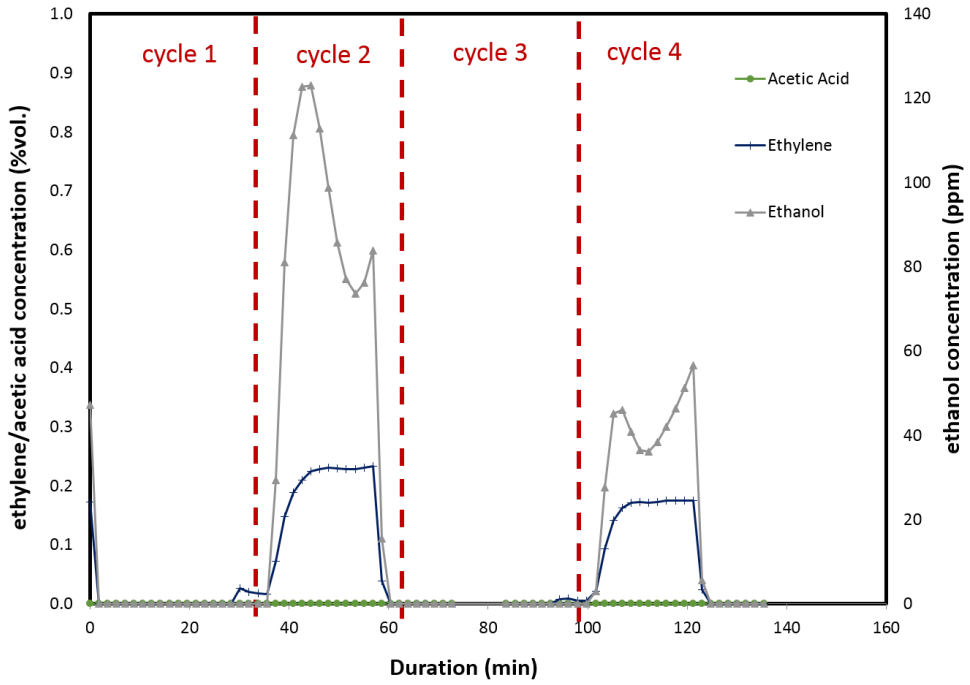

Figure 9. Minor components from process. Cycles 2 and 4 pass through a Pd/Co on SiO_2 catalyst. Cycles 1 and 3 pass through a reactor with no catalyst. Product formation is visible with catalyst.

In our experiments, higher pressure resulted in higher product formation. For example, when a $Pt/Co/TiO_2$ catalyst was used (in tests 2 and 3, from Table 2), there was a methanol peak which was visible at 150 psig but not at lower pressures.

One side reaction which was present was CO_2 hydrogenation (methanation), which produced methane from CO_2 and hydrogen, shown below. This is an undesirable side reaction and is directly related to the hydrogen concentration (at higher H_2 concentrations, CH_4 production was increased). The hydrogen output inversely tracked the ethylene production, indicating that hydrogen is consumed in the production of ethylene.

Methanation reaction: $CO_2 + 4H_2 \rightarrow CH_4 + 2H_2O$

The impacts of process variables (temperature, pressure, water concentration, and switch time) were investigated. Temperature was varied from 150-300^oC. Pressure was varied from 0 – 250 psig. Switch time was varied from 200-1500s, and water concentration was varied from 0-0.25 mL/min. A summary of the results from parametric tests that were completed is shown in Table 3. An example of some test data from tests 21, 22, 26, and 27 is shown in Figure 10. The catalyst in reactor 1 was $Pd\text{-}Co/SiO_2$ and reactor 2 contained Pd/SiO_2 mixed with Co/SiO_2. Therefore, every 900s (the designated valve switching time) corresponds to the switching between the two catalysts. At 300°C, 130 ppm of ethylene was produced with a bimetallic catalyst. At 250^oC, 16 ppm of ethylene was produced. Ethanol was produced in concentrations of ~1 ppm.

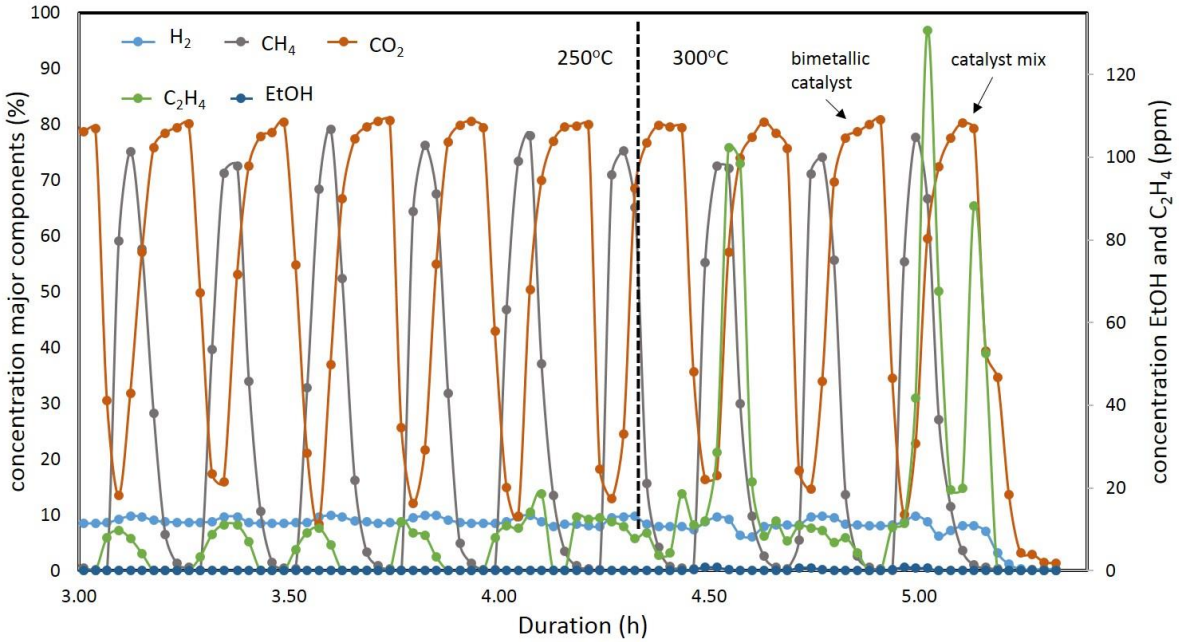

Figure 10. Gas composition data for runs at 250°C and 300°C using a bimetallic Pd-Co/SiO_2 catalyst and a catalyst mixture of Pd/SiO_2 and Co/SiO_2.

The impact of water is shown in Figures 11 and 12. These results are for tests 36-39 (from Table 3), with a bimetallic Pd-Co/SiO_2 catalyst and a catalyst mixture of Pd/SiO_2 and Co/SiO_2. Ethanol and ethylene were produced in concentrations up to 28 ppm and 1360 ppm, respectively. The introduction of water decreased the concentrations of ethylene and ethanol in the product. Some tests produced ethanol and methanol in the condensate which was recovered after the test. This was detected with the GC/MS, and an example of the data is shown in Figure 13.

None of the tests produced conversions that were high enough to make the process commercially viable. The products, ethanol, methanol, and ethylene were only visible at higher reaction pressures. However, due to the very low conversion, it was difficult to quantify the impacts of reaction conditions outside of experimental error.

Due to extremely low conversion of CO_2, we determined the above method to be ineffective at producing acetic acid. As a result, we changed our focus to dry reforming of CH_4 with CO_2. This reaction can also produce acetic acid via the traditional two-step process where the syngas product (CO and H_2) is used to produce methanol, which subsequently reacts with CO to produce acetic acid. The experimental methods and outcomes of the dry reforming work are discussed in the following section.

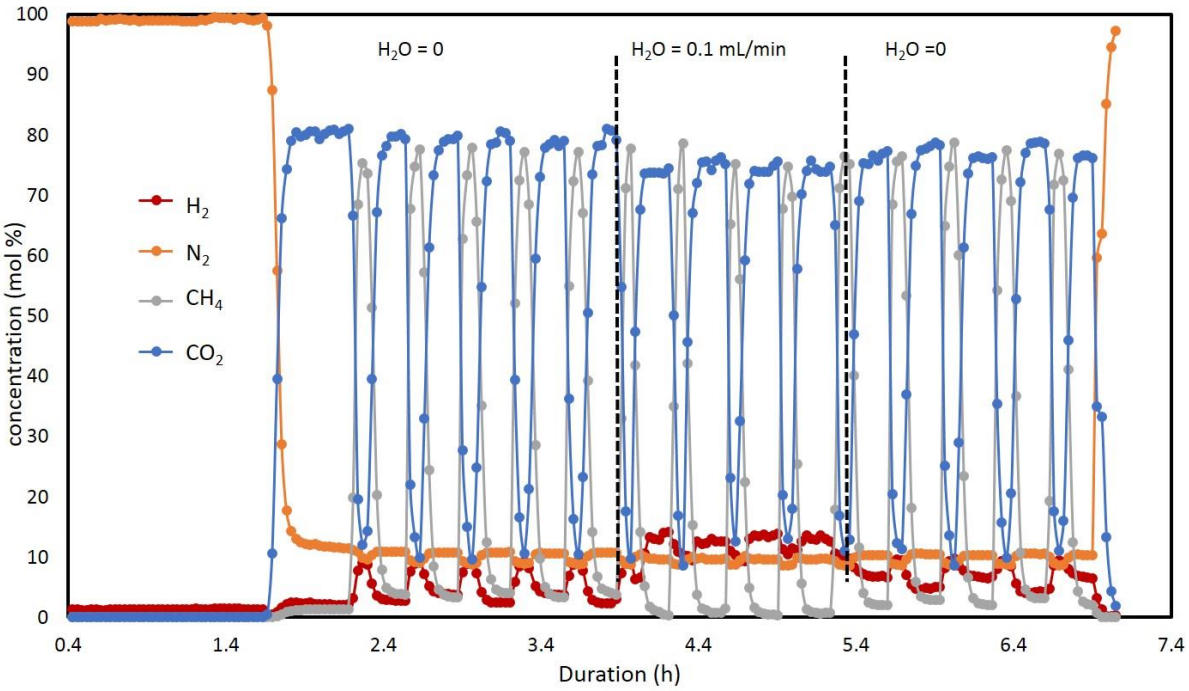

Figure 11. Major components from experiments 36-39, using a bimetallic Pd-Co/SiO_2 catalyst and a catalyst mixture of Pd/SiO_2 and Co/SiO_2. Reaction temperature is 300°C and pressure is 250psig.

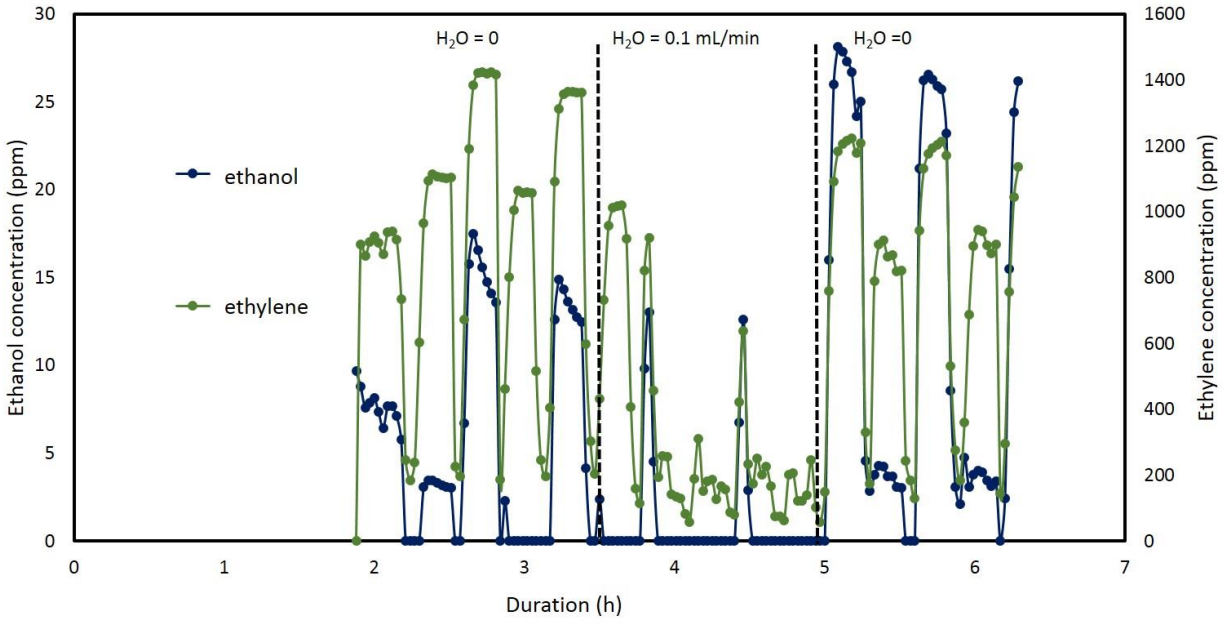

Figure 12. Minor components from experiments 36-39, using a bimetallic Pd-Co/SiO_2 catalyst and a catalyst mixture of Pd/SiO_2 and Co/SiO_2. Reaction temperature is 300°C and pressure is 250psig.

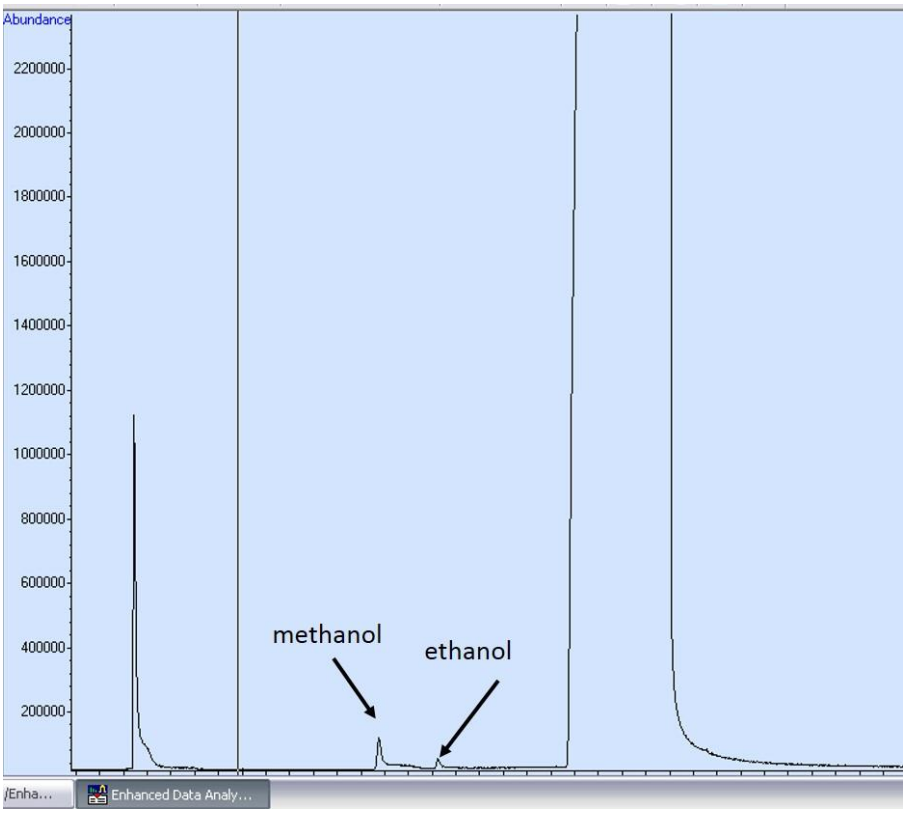

Figure 13. Methanol and ethanol peaks in GC/MS condensate from tests 48-55. Tests were done continuously so condensate from these runs are combined in knock out, and recovered after all tests.

Table 3: Summary of parametric tests performed.

Test	Catalyst	Temp (°C)	Pressure (psig)	Flow Rates (sccm)								Switch time (min)	Products		Liquid product
				CH_4	H_2	H_2O	N_2	CO_2	H_2	H_2O	N_2		Ethylene* (ppm)	Ethanol* (ppm)	
1	$Pd/Co/TiO_2$	150	200	133	13	0.01	15	133	13	0.005	15	15	38	ND	
2	$Pd/Co/TiO_2$	200	200	133	13	0.01	15	133	13	0.005	15	15	43	0.8	
3	$Pd/Co/TiO_2$	250	200	133	13	0.01	15	133	13	0.005	15	15	47	ND	
4	$Pd/Co/TiO_2$	200	200	133	13	0	15	133	13	0.01	15	15	9	ND	
5	$Pd/Co/TiO_2$	200	200	133	13	0.01	15	133	13	0.01	15	15	10	ND	
6	$Pd/Co/TiO_2$	200	200	133	13	0.05	15	133	13	0.05	15	15	10	ND	
7	$Pd/Co/TiO_2$	200	200	133	13	0.1	15	133	13	0.1	15	15	9	ND	
8	$Pd/Co/TiO_2$	200	200	133	13	0.1	15	133	13	0.1	15	15	13	0.5	
9	$Pd/Co/TiO_2$	200	160	133	13	0.1	15	133	13	0.1	15	15	13	0.5	
10	$Pd/Co/TiO_2$	200	110	133	13	0.1	15	133	13	0.1	15	15	3	0.5	
11	$Pd/Co/TiO_2$	200	60	133	13	0.1	15	133	13	0.1	15	15	0	0.4	
12	$Pd/Co/SiO_2$	190	250	133	13	0.1	15	133	13	0.1	15	15	9	ND	methanol detected in collective liquid condensate (70 ppm)
13	$Pd/Co/SiO_2$	190	200	133	13	0.1	15	133	13	0.1	15	15	7	ND	
14	$Pd/Co/SiO_2$	190	100	133	13	0.1	15	133	13	0.1	15	15	7	ND	
15	Pd/SiO_2 + Co/SiO_2	190	250	133	13	0.1	15	133	13	0.1	15	15	9	ND	
16	Pd/SiO_2 + Co/SiO_2	190	200	133	13	0.1	15	133	13	0.1	15	15	9	ND	

17	Pd/SiO_2 + Co/SiO_2	190	100	133	13	0.1	15	133	13	0.1	15	15	6	ND	
18	$Pd/Co/SiO_2$	150	250	133	13	0.1	15	133	13	0.1	15	15	8	0.4	methanol detected in collective liquid condensate (18 ppm)
19	$Pd/Co/SiO_2$	150	250	133	13	0.1	15	133	13	0.1	15	15	8	0.4	
20	$Pd/Co/SiO_2$	200	250	133	13	0.1	15	133	13	0.1	15	15	8	0.4	
21	$Pd/Co/SiO_2$	250	250	133	13	0.1	15	133	13	0.1	15	15	9	ND	
22	$Pd/Co/SiO_2$	300	250	133	13	0.1	15	133	13	0.1	15	15	11	0.3	
23	Pd/SiO_2 + Co/SiO_2	150	250	133	13	0.1	15	133	13	0.1	15	15	8	0.4	
24	Pd/SiO_2 + Co/SiO_2	150	250	133	13	0.1	15	133	13	0.1	15	15	8	0.4	
25	Pd/SiO_2 + Co/SiO_2	200	250	133	13	0.1	15	133	13	0.1	15	15	10	0.4	
26	Pd/SiO_2 + Co/SiO_2	250	250	133	13	0.1	15	133	13	0.1	15	15	9	ND	
27	Pd/SiO_2 + Co/SiO_2	300	250	133	13	0.1	15	133	13	0.1	15	130	14	0.3	
28	$Pd/Co/SiO_2$	300	250	133	13	0	15	133	13	0	15	15	938	3	methanol detected in collective liquid condensate (9 ppm)
29	$Pd/Co/SiO_2$	300	250	133	13	0	15	133	26	0	15	15	953	ND	
30	$Pd/Co/SiO_2$	300	250	133	13	0	15	133	26	0	15	25	1078	3	
31	$Pd/Co/SiO_2$	300	250	133	13	0.1	15	133	26	0.1	15	25	176	ND	
32	Pd/SiO_2 + Co/SiO_2	300	250	133	13	0	15	133	13	0	15	15	699	0.3	
33	Pd/SiO_2 + Co/SiO_2	300	250	133	13	0	15	133	26	0	15	15	1125	4	
34	Pd/SiO_2 + Co/SiO_2	300	250	133	13	0	15	133	26	0	15	25	1064	4	
35	Pd/SiO_2 + Co/SiO_2	300	250	133	13	0.1	15	133	26	0.1	15	25	911	4	
36	$Pd/Co/SiO_2$	300	250	133	13	0	15	133	26	0	15	20	1019	2	

37	$Pd/Co/SiO_2$	300	250	133	13	0.1	15	133	26	0.1	15	20	310	ND	methanol detected in collective liquid condensate (7 ppm)
38	Pd/SiO_2 + Co/SiO_2	300	250	133	13	0	15	133	26	0	15	20	1355	28	
39	Pd/SiO_2 + Co/SiO_2	300	250	133	13	0.1	15	133	26	0.1	15	20	637	13	
40	$Pd/Co/SiO_2$	300	250	133	13	0	15	133	13	0	15	20	803	7	
41	$Pd/Co/SiO_2$	300	250	0	13	0	145	133	13	0	15	20	779	7	
42	$Pd/Co/SiO_2$	300	250	0	13	0	145	133	39	0	15	20	1081	5	
43	$Pd/Co/SiO_2$	300	250	133	13	0	15	133	39	0	15	20	1238	5	
44	Pd/SiO_2 + Co/SiO_2	300	250	133	13	0	15	133	13	0	15	20	749	22	
45	Pd/SiO_2 + Co/SiO_2	300	250	0	13	0	145	133	13	0	15	20	681	21	
46	Pd/SiO_2 + Co/SiO_2	300	250	0	13	0	145	133	39	0	15	20	1142	32	
47	Pd/SiO_2 + Co/SiO_2	300	250	133	13	0	15	133	39	0	15	20	1112	30	
48	$Pd/Co/SiO_2$	290	250	133	13	0	15	133	26	0	15	20	998	ND	methanol detected in collective liquid condensate (33 ppm); Ethanol detected in collective condensate (6 ppm)
49	$Pd/Co/SiO_2$	290	250	133	13	0.01	15	133	26	0.01	15	20	875	ND	
50	$Pd/Co/SiO_2$	290	250	133	13	0.05	15	133	26	0.05	15	20	505	ND	
51	$Pd/Co/SiO_2$	290	250	133	13	0.1	15	133	26	0.1	15	20	280	ND	
52	Pd/SiO_2 + Co/SiO_2	290	250	133	13	0	15	133	26	0	15	20	928	ND	
53	Pd/SiO_2 + Co/SiO_2	290	250	133	13	0.01	15	133	26	0.01	15	20	994	ND	
54	Pd/SiO_2 + Co/SiO_2	290	250	133	13	0.05	15	133	26	0.05	15	20	217	ND	
55	Pd/SiO_2 + Co/SiO_2	290	250	133	13	0.1	15	133	26	0.1	15	20	104	ND	

56	$Pd/Co/TiO_2$	150	250	133	13	0.1	13	133	13	0.1	15	15	0	ND	
57	$Pd/Co/TiO_2$	150	250	133	13	0.1	13	133	13	0.1	15	3.3	26	ND	
58	$Pd/Co/TiO_2$	150	250	133	27	0.1	13	133	27	0.1	15	3.3	30	ND	
59	$Pd/Co/TiO_2$	150	150	133	27	0.1	13	133	27	0.1	15	3.3	32	ND	
60	$Pd/Co/TiO_2$	150	150	133	27	0.2	13	133	27	0.2	15	3.3	28	ND	
61	$Pd/Co/TiO_2$	150	atm	133	27	0.2	13	133	27	0.2	15	3.3	26	ND	
62	$Pd/Co/TiO_2$	150	atm	133	27	0.2	13	133	27	0.2	15	3.3	26	ND	
63	$Pd/Co/TiO_2$	150	atm	133	27	0.25	13	133	27	0.25	15	3.3	28	ND	
64	$Pd/Co/TiO_2$	150	atm	133	27	0	13	133	27	0	15	3.3	30	ND	
65	Pd/TiO_2 + Co/TiO_2	150	250	133	13	0.1	13	133	13	0.1	15	15	0	ND	
66	Pd/TiO_2 + Co/TiO_2	150	250	133	13	0.1	13	133	13	0.1	15	3.3	28	ND	
67	Pd/TiO_2 + Co/TiO_2	150	250	133	27	0.1	13	133	27	0.1	15	3.3	30	ND	
68	Pd/TiO_2 + Co/TiO_2	150	150	133	27	0.1	13	133	27	0.1	15	3.3	32	ND	
69	Pd/TiO_2 + Co/TiO_2	150	150	133	27	0.2	13	133	27	0.2	15	3.3	28	ND	
70	Pd/TiO_2 + Co/TiO_2	150	atm	133	27	0.2	13	133	27	0.2	15	3.3	26	ND	
71	Pd/TiO_2 + Co/TiO_2	150	atm	133	27	0.2	13	133	27	0.2	15	3.3	26	ND	
72	Pd/TiO_2 + Co/TiO_2	150	atm	133	27	0.25	13	133	27	0.25	15	3.3	28	ND	
73	Pd/TiO_2 + Co/TiO_2	150	atm	133	27	0	13	133	27	0	15	3.3	30	ND	

* Concentrations are outside of calibration limits, so these values should serve as an estimate, demonstrating trends. ND = not detected by micro gc

3.2 Dry Reforming of CO_2 and CH_4

3.2.1 Catalyst Preparation and Characterization

Nickel (Ni) nanoparticle catalysts supported on two different substrates were synthesized by atomic layer deposition (ALD) using bis(cyclopentadienyl)nickel ($NiCp_2$) and H_2 as precursors at 300 ºC. The prepared catalysts were used to catalyze the dry reforming of methane (DRM) reaction. The ALD chemistry is schematically shown in Figure 14. ALD is a self-limiting and self-terminating gas phase deposition technique that has been successfully demonstrated for the synthesis of metal nanoparticles (e.g., Pd and Pt) on different substrates [1, 2]. In this study, five cycles of Ni ALD were applied on both substrates. Two nickel catalysts were synthesized, labeled as Catalyst A and Catalyst B.

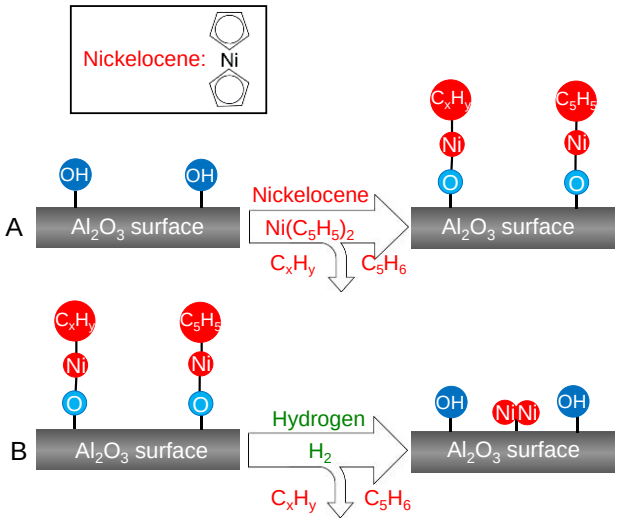

Figure 14. Schematic representation of one cycle of Ni ALD using $NiCp_2$ and H_2 as precursors.

The Ni content was determined by inductively coupled plasma-atomic emission spectroscopy (ICP–AES). The Ni loadings on Catalyst A and Catalyst B were 2.91 wt.% and 0.12 wt.%, respectively. Transmission electron microscopy (TEM) was used to verify that extremely small Ni nanoparticles (~3 nm) were uniformly deposited on the surface of substrates.

3.2.2 Dry reforming test setup and general procedure

The catalytic reactor system is shown in Figure 16 and the process flow diagram is shown in Figure 17. Different amounts of various catalysts were loaded into a quartz tube reactor (10 mm diameter) to keep the Ni content consistent (~0.74 mg). Quartz wool was employed to support the catalysts. A thermocouple was used to measure the temperature in the catalyst bed. Both catalysts were reduced with 20% H_2 and 80% Ar (with a total flow rate of 100 sccm) at 700 °C for 1 hour before the DRM reaction. The reactions were carried out at atmosphere pressure. CH_4 and CO_2 (CH_4: CO_2 = 1:1, with a total flow rate of 60 sccm) were introduced into the reactor at different temperatures for the DRM reaction. The gas flow rates were controlled by MKS® mass flow controllers. The reaction products were analyzed by an online gas chromatograph (SRI 8610C) equipped with a 6-foot HAYESEP D column, a 6-foot MOLECULAR SIEVE 13X column, and a thermal conductivity detector (TCD). Some other detailed catalyst test conditions are listed in Table 4.

Figure 16. Photo of the packed bed catalytic reactor at Missouri S&T.

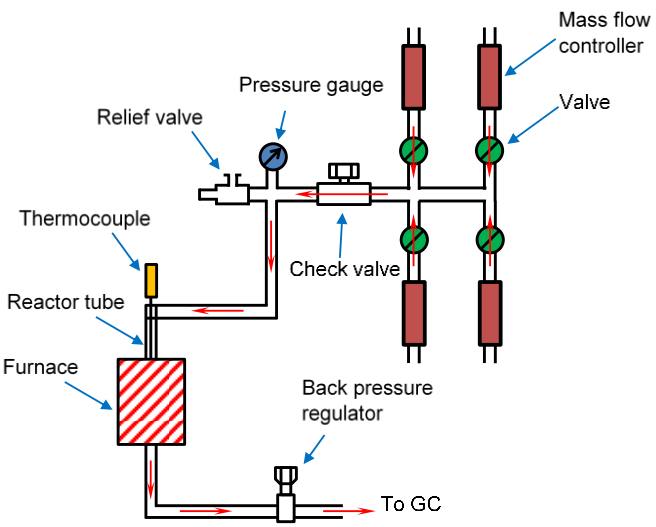

Figure 17. Process flow diagram of the packed bed catalytic reactor at Missouri S&T

Table 4. Reaction conditions for catalyst testing.

Catalysts	Reactants (CO_2/CH_4) [%]	T [°C]	Length of test [hour]	Space velocity* [mL/min/$g_{catalyst}$]	Regeneration **	Status
Catalyst A (1-2 wt.% Ni)	50/50	850	48	780	No	Finished
Catalyst A (1-2 wt.% Ni)	50/50	800	48	780	No	Finished
Catalyst A (1-2 wt.% Ni)	50/50	750	48	780	No	Finished
Catalyst A (1-2 wt.% Ni)	50/50	700	48	780	No	Finished
Catalyst A (1-2 wt.% Ni)	50/50	850 or 700	>300	780	Yes	Finished
Catalyst B (0.1-0.2 wt.% Ni)	50/50	850	48	80	No	Finished
Catalyst B (0.1-0.2 wt.% Ni)	50/50	800	48	80	No	Finished
Catalyst B (0.1-0.2 wt.% Ni)	50/50	750	48	80	No	Finished
Catalyst B (0.1-0.2 wt.% Ni)	50/50	700	48	80	No	Finished
Catalyst B (0.1-0.2 wt.% Ni)	50/50	850 or 700	>300	80	Yes	Finished

* When we calculated space velocity, here $g_{catalyst}$ is based on Ni metal catalyst plus alumina support.

3.2.3 Results of dry reforming testing

The results for both Catalyst A and Catalyst B catalysts with no regeneration at different temperatures are shown in Figure 18. The main components in the product are CH_4, CO_2, CO, H_2 and H_2O. Water is produced via the reverse water-gas shift reaction ($CO_2 + H_2 \rightleftharpoons H_2O + CO$). The mole fractions of the different components were determined by gas chromatograph. For example, for the 1st point of Catalyst B catalyzed reaction in Figure 18, the molar ratio of H_2: CO: CH_4: H_2O is 14.6: 22.7: 1: 0.4. The CO_2 cannot be detected by TCD, since Ar was used as carrier gas and the thermal conductivities of Ar and CO_2 are very close. However, because the dry reforming reaction has a 1:1 ratio of CO_2:CH_4, and the reverse water gas shift reaction only has a small extent of reaction (since the ratio of water to H_2 is 0.4:14.6), we can deduce that the conversion of CO_2 is slightly higher than the methane conversion.

As shown in Figure 18, Catalyst B catalyst showed much higher activity as compared to the Catalyst A. The exact reason for the higher activity at 800 °C as compared to that at 850 °C is not clear.

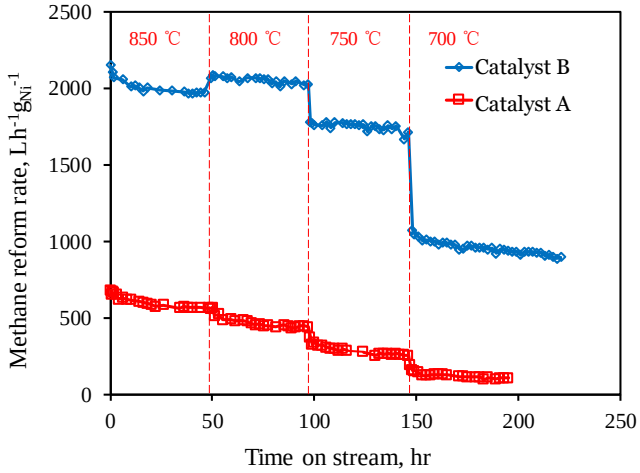

Figure 18. Methane reforming rate of dry reforming of methane catalyzed by nickel catalysts without regeneration at different temperatures.

Later, both catalysts were tested for 3 cycles (here cycle means one test at different reaction temperatures without regeneration in between reaction temperatures). The catalyst was regenerated after each cycle. The results are shown in Figures 19 and 20. As shown in Figure 19, Catalyst A showed similar performance as compared to the previous test (Figure 18) at 850 °C and 700 °C in the 1st cycle. In the 2nd and 3rd cycles, the catalyst showed lower performance which could be due to the sintering of Ni nanoparticles. As shown in Figure 20, Catalyst B showed similar performance at 850 °C as compared to the previous test (Figure 18) in the 1st cycle. The methane reforming rate at 700 °C was higher as compared to the previous test. However, the rate of methane reforming decreased more rapidly. In the 2nd and 3rd cycles, the catalyst showed similar performance. The catalyst showed slightly lower activity as compared to the 1st cycle at 850 °C, which could be due to the sintering of Ni nanoparticles in the 1st cycle of reaction. The fact that the catalyst showed similar activity at 700 °C indicates that the catalyst could show repeatable performance after regeneration.

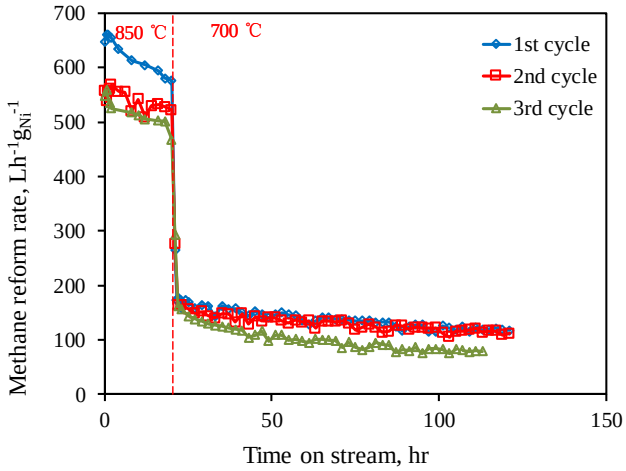

Figure19. Methane reforming rate of three cycles of dry reforming of methane catalyzed by Catalyst A with regeneration between each cycle.

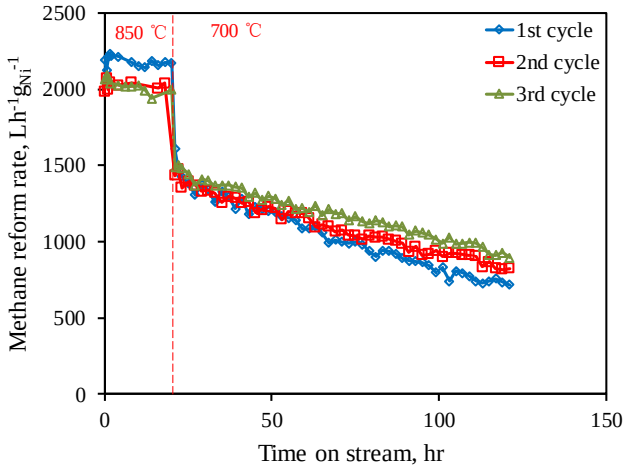

Figure 20. Methane reforming rate of three cycles of dry reforming of methane catalyzed by Catalyst B with regeneration between each cycle.

4 Greenhouse Gas and Non-GHG impacts

The proposed technology offers a mechanism to utilize CO_2 that would otherwise be released to the atmosphere from sources such as power plants or landfills. In the case of a power plant, CO_2 reacts with methane (from natural gas) to produce syngas which can then be used for chemical synthesis. If the syngas is used to produce acetic acid (via a methanol intermediate), this would result in 0.73 kg CO_2 utilized per kg of acetic acid. If the feedstock for the process is landfill gas, then this would result in 0.73 kg CO_2 and 0.27 kg of methane utilized per kg of acetic acid produced, that would otherwise be released to the atmosphere. The global demand for acetic acid

was 10 Mmta in 2011.[21] This corresponds to 7.3Mmta of CO_2 utilized. The acetic acid market is expected to grow to 15 Mmta by 2020, corresponding to 11 Mmta of CO_2 utilized from acetic acid production.[21] If the syngas is made from CO_2 captured from a power plant with natural gas as a co-reactant, then half of the CO_2 in the final product would be avoided emissions (the natural gas does not count as avoided GHG emissions), so this would offset 6.5 Mmta of CO_2 based on 2020 estimates. The demand for acetic acid is not very high compared to the CO_2 that is released for power plants. Therefore, it would also be useful to use the methanol produced from the process, since methanol has a much larger market. For example, in 2015, the global methanol demand was 70 million metric tons.[22] This means that with landfill gas a feedstock, one ton of methanol would consume 1.9 ton of greenhouse gases (CO_2 and CH_4), with additional CO being produced. For a methanol market of 70 Mmta, this is a GHG reduction of 131 million metric tons in one year. Over 10 years, this would result in 1,310 million metric tons of GHG reductions. If the dry reforming reaction is based on CO_2 captured from a power plant and CH4 from natural gas, then only the CO_2 is counted towards GHG emissions reductions, resulting in 1.4 ton of GHG emissions reduction per ton of methanol. Again, there is additional CO produced which could be used for synthesis of other chemicals. In one year, this corresponds to 98 million metric tons of GHG reductions

Dry reforming of methane: $CO_2 + CH_4 \rightarrow 2CO + 2H_2$

Methanol synthesis: $CO + 2H_2 \rightarrow CH_3OH$

Acetic acid synthesis: $CH_3OH + CO \rightarrow CH_3COOH$

5 Overall conclusions

The research done during this project investigated ways to utilize CO_2 using methane as a co-reactant for production of useful products. The initial objective was to produce acetic acid and ethanol directly from CO_2 and CH_4 using a simulated moving bed reactor. While many different catalysts were investigated for this reaction, and extensive reaction conditions were investigated, the product yield was not significant to make the process viable. As a result, we pursued the dry reforming reaction using a nickel catalyst synthesized by atomic layer deposition (ALD), on a stable support. The catalyst experienced deactivation, as is expected with this reaction. After regeneration, the catalyst showed lower performance in the second cycle compared to the first cycle. However, cycles 2 and 3 showed similar performance, suggesting that stable activity may

be achievable with frequent regenerations. More cycle testing would be necessary in order to verify the long term stability of the catalyst. There have not been any publications of this work at the time of submission of this report.

6 Next Steps

Before this technology can be commercialized, further testing would need to be done in order to understand the long term stability of the catalyst. This technology would be applicable in two scenarios. First, it is appropriate for production of syngas from biogas, for example from a landfill or from anaerobic digestion. In that case, the biogas would need to be cleaned to remove sulfur compounds, or other impurities that might poison the catalyst. The syngas could then be used to produce methanol, formic acid, or acetic acid. Alternatively, CO_2 could be captured from a coal or natural gas fired power plant and mixed with natural gas. The mixture would then undergo the dry reforming process, producing syngas. As of right now, the next steps are to further evaluate and develop the catalyst. The results of these tests will be communicated by publishing the results in a scientific journal.

7 Participants and Collaborating Organizations

The dry reforming work was performed by Professor Xinhua Liang's group at Missouri University of Science and Technology.

8 Bibliography

1. Jones, J. H. “The Cativa Process for the Manufacture of Acetic Acid”, Platinum Metals Rev., 2000, 44, (3), 94.
2. García-Diéguez, M.; Pieta, I. S.; Herrera, M. C.; Larrubia, M. A.; Malpartida, I.; Alemany, L. J., Transient study of the dry reforming of methane over Pt supported on different γ-Al_2O_3. *Catalysis Today* **2010,** 149, (3-4), 380-387.
3. Luo, J. Z.; Yu, Z. L.; Ng, C. F.; Au, C. T., CO_2/CH_4 reforming over Ni–La_2O_3/5A: An investigation on carbon deposition and reaction steps. *Journal of Catalysis* **2000,** 194, (2), 198-210.
4. Mark, M. F.; Maier, W. F., CO_2-reforming of methane on supported Rh and Ir catalysts. *Journal of Catalysis* **1996,** 164, (1), 122-130.
5. Bradford, M. C. J.; Vannice, M. A., CO_2 reforming of CH_4 over supported Pt catalysts. *Journal of Catalysis* **1998,** 173, (1), 157-171.
6. Schulz, P. G.; Gonzalez, M. G.; Quincoces, C. E.; Gigola, C. E., Methane reforming with carbon dioxide. The behavior of Pd/α-Al_2O_3 and Pd-CeOx/α-Al_2O_3 catalysts. *Industrial & Engineering Chemistry Research* **2005,** 44, (24), 9020-9029.
7. Carrara, C.; Munera, J.; Lombardo, E. A.; Cornaglia, L. M., Kinetic and stability studies of Ru/La_2O_3 used in the dry reforming of methane. *Topics in Catalysis* **2008,** 51, (1-4), 98-106.
8. Barroso-Quiroga, M. M.; Castro-Luna, A. E., Catalytic activity and effect of modifiers on Ni-based catalysts for the dry reforming of methane. *International Journal of Hydrogen Energy* **2010,** 35, (11), 6052-6056.
9. Jones, G.; Jakobsen, J. G.; Shim, S. S.; Kleis, J.; Andersson, M. P.; Rossmeisl, J.; Abild-Pedersen, F.; Bligaard, T.; Helveg, S.; Hinnemann, B., First principles calculations and experimental insight into methane steam reforming over transition metal catalysts. *Journal of Catalysis* **2008,** 259, (1), 147-160.
10. Hou, Z. Y.; Chen, P.; Fang, H. L.; Zheng, X. M.; Yashima, T., Production of synthesis gas via methane reforming with CO_2 on noble metals and small amount of noble-(Rh-) promoted Ni catalysts. *International Journal of Hydrogen Energy* **2006,** 31, (5), 555-561.
11. Wang, R.; Xu, H. Y.; Liu, X. B.; Ge, Q. J.; Li, W. Z., Role of redox couples of $Rh^0/Rh^{\delta+}$ and Ce^{4+}/Ce^{3+} in CH_4/CO_2 reforming over Rh–CeO_2/Al_2O_3 catalyst. *Applied Catalysis A: General* **2006,** 305, (2), 204-210.

12. George, S. M., Atomic layer deposition: An overview. *Chemical Reviews* **2010,** 110, (1), 111-131.
13. Liang, X. H.; Zhou, Y.; Li, J. H.; Weimer, A. W., Reaction mechanism studies for platinum nanoparticle growth by atomic layer deposition. *Journal of Nanoparticle Research* **2011,** 13, (9), 3781-3788.
14. King, D. M.; Liang, X. H.; Weimer, A. W., Functionalization of fine particles using atomic and molecular layer deposition. *Powder Technology* **2012,** 221, 13-25.
15. Shang, Z. Y.; Li, S. G.; Li, L.; Liu, G. Z.; Liang, X. H., Highly active and stable alumina supported nickel nanoparticle catalysts for dry reforming of methane. *Applied Catalysis B: Environmental* **2017,** 201, 302-309.
16. Santos, P. S.; Santos, H. S.; Toledo, S. P., Standard transition aluminas. Electron microscopy studies. *Materials Research* **2000,** 3, (4), 104-114.
17. Huang, W. Sun, W. Z., Li, F. Efficient Synthesis of Ethanol and Acetic Acid from Methane and Carbon Dioxide with a Continuous, Stepwise Reactor. AIChE Journal, **2010**, 56, 5, 1279-1284.
18. L. H. Song, Z. F. Yan and S. K. Shen, Prepr. Pap.-Am. Chem. Soc., Div. Fuel Chem. 2004, 49 (1), 402
19. D. Schroder and J. Roithova, Angew. Chem. Int. Ed. 2006 45 5705-5708
20. M. M. Koranne and D. W. Goodman, Catalysis Letters, 1995, 30 219-234
21. GBI Research, report, "Acetic Acid Global Market 2020"
22. Methanol Institute, available online at http://www.methanol.org/the-methanol-industry/, accessed online Sept. 30, 2016.